arXiv:1609.02474v1 [cond-mat.mes-hall] 8 Sep 2016

Thermopower of molecular junctions: Tunneling to hopping crossover in DNA

Roman Korol,[1] Michael Kilgour,[1] and Dvira Segal[1, a)]
Chemical Physics Theory Group, Department of Chemistry, University of Toronto, 80 St. George Street Toronto, Ontario, Canada M5S 3H6

(Dated: 9 September 2016)

We study the electrical conductance G and the thermopower S of single-molecule junctions, and reveal signatures of different transport mechanisms: off-resonant tunneling, on-resonant coherent (ballistic) motion, and multi-step hopping. These mechanisms are identified by studying the behavior of G and S while varying molecular length and temperature. Based on a simple one-dimensional model for molecular junctions, we derive approximate expressions for the thermopower in these different regimes. Analytical results are compared to numerical simulations, performed using a variant of Büttiker's probe technique, the so-called voltage-temperature probe, which allows us to phenomenologically introduce environmentally-induced elastic and inelastic electron scattering effects, while applying both voltage and temperature biases across the junction. We further simulate the thermopower of GC-rich DNA molecules with mediating A:T blocks, and manifest the tunneling-to-hopping crossover in both the electrical conductance and the thermopower, in accord with measurements by Y. Li *et al.*, Nature Comm. 7, 11294 (2016).

I. INTRODUCTION

Complementing electrical conductance measurements, the thermoelectric effect can serve as an accurate probe to investigate the transport characteristics of molecular junctions[1,2]. Specifically, measurements of the thermopower of single organic molecules reveal whether electrons or holes are the primary charge carriers[3]. The thermopower can further reveal relative orbital level-alignment[4–6], and pinpoint transport mechanisms, in support of electrical conductance measurements[7–12].

Thermoelectric devices are attractive for applications requiring heat to work conversion without moving parts, a task for which nanoscale systems are particularly suitable due to their sharp energy level structure, key for achieving high thermoelectric efficiency[13,14]. The thermoelectric figure-of-merit of molecular junctions, ZT, is defined as $ZT = GS^2T/\kappa$, with G as the electrical conductance, S the thermopower, and κ the thermal conductance, comprising both electron and phonon contributions. Understanding the behavior of G and S is therefore crucial for applications requiring enhanced heat to work conversion efficiency.

Measurements of the charge transfer rate and electrical conductance of single-molecule junctions and self assembled monolayers have revealed three primary limiting mechanisms[15,16]: phase-coherent off-resonance "deep" tunneling (superexchange), coherent on-resonance (ballistic) conduction, and sequential incoherent hopping. In the deep tunneling regime the electrical conductance decreases exponentially with distance, becoming insignificant in long molecules. Further, in this regime the conductance is independent of the temperature of the leads[15,16].

In contrast, ballistic conduction is largely insensitive to molecular length, and is thermally activated according to the Fermi distribution of the metal electrodes[17,18]. If transport charges interact with "environmental" (internal of external) degrees of freedom such as phonons, long-range electron transfer is dominated by thermally activated incoherent hopping processes. Such a multi-step hopping mechanism is characterized by a linear enhancement of resistance with molecular length.

The transition from off-resonant tunneling to hopping, or alternatively, to ballistic dynamics, has been resolved experimentally by studying the distance and temperature dependence of the electrical conductance. Such experiments were conducted within a wide array of organic molecules, see e.g. Refs.[17–20], and biomolecules, e.g.[21,22], revealing a consistent picture, as described above. In contrast, experiments of the thermoelectric effect in single organic molecules have been primarily limited to situations in which off-resonant tunneling was the primary transport mechanism[2,3]. In this regime, the Fermi energy is located deep in the gap between the HOMO and the LUMO. Landauer theory then predicts that as the electrical conductance G decays exponentially with molecular length, the thermopower S should see a linear enhancement[2]. As well, in this deep tunneling regime S should scale linearly with the leads' temperature. These predictions were verified experimentally by several groups[2,8,10].

While the behavior of the thermopower has thus far been assessed primarily in the deep tunneling limit, a recent study of DNA molecules reported the crossover from tunneling to hopping behavior, observed simultaneously through the electrical conductance and the thermopower[12]. Several DNA sequences were evaluated in this work: In alternating $(GC)_n$ sequences, site-to-site hopping is expected to be the dominant transport mechanism, with each purine base serving as a hopping site for holes. These sequences manifested an ohmic behavior, with the resistance growing linearly, and the thermopower decaying weakly-monotonically with length n. In contrast, GC-rich sequences with mediating A:T

a) Electronic mail: dsegal@chem.utoronto.ca

blocks, acting as a tunneling barrier, were demonstrated to support superexchange behavior for short molecules, with the conductance decreasing exponentially with the barrier width. Here, A, G, C and T are the adenine, guanine, cytosine and thymine bases, respectively. By extending the A:T block, the full crossover from tunneling to hopping was realized in the conductance. At the same time, the thermopower exhibited non-monotonic behavior: It was linearly enhanced in the deep tunneling regime (as expected), but when hopping conductance was argued to dominate, it dropped down below the superexchange value, and then was mostly insensitive to length. This intriguing behavior calls for theoretical work.

What theoretical-computational approaches are available to simulate G and S, which can explore the full tunneling to hopping crossover in molecular junctions? Focusing on works reporting on both G and S, we note that most computational studies of linear-response transport coefficients in single molecules are limited to the coherent limit[23], using the Landauer formula with parameters derived from first principle calculations[24–34], or other coherent-transport approaches[35]. Effects of vibrations on the thermopower were assessed using scattering approaches[36,37], or perturbatively using non-equilibrium Green's function (NEGF)[38–43] or quantum master equation (QME) methods[42–46]. However, given the computational cost, such treatments are limited to describe rather small systems with few (1-2) molecular electronic orbitals and 1-2 primary vibrational modes. Thus, while scattering methods, the NEGF technique, or QME tools can be used to identify vibrationally-assisted transport effects, they cannot be feasibly employed to reveal the full crossover from tunneling dynamics to multi-step hopping as induced by electron-vibration interaction processes.

The Redfield equation of motion, which does not explicitly include particular molecular vibrations, can be used to describe charge transport in extended-interacting systems[15]. In this method, the information from the thermal environment is encapsulated within Fourier transforms of bath correlation functions which can be generated to mimic thermalized vibrational effects. Based on a (phenomenological) generalization of the Landauer equation to include inelastic effects, the Redfield approach was used in Ref.[47] to uncover the full tunneling-to-hopping crossover concurrently in the behavior of G and S. This approach however relies on several significant assumptions: (i) The inelastic transmission probability, which allows for energy exchange with the environment, was conjectured to exist. The Landauer framework was then assumed to hold, predicated on the existence of single quasi-particle scattering states. (ii) Certain voltage and temperature profiles were presumed to develop across the junction. Also, as we discuss after Eq. (19), the ballistic contribution was incorrectly identified as hopping conduction in some places in Ref.[47]. It is thus necessary to develop a new framework, based on more solid grounds, for simulating the thermopower in systems affected by environmental interactions.

The Landauer-Büttiker probe (LBP) method offers an alternative route for introducing environmental effects into charge transport dynamics at low cost. The method is particularly appealing since it allows the study of a broad range of systems, from single-atom junctions up to the thermodynamic limit. In this technique, incoherent elastic and inelastic scattering effects are included in a phenomenological manner, by augmenting the non-interacting electronic Hamiltonian with probe terminals through which electrons lose their phase memory and (possibly) exchange energy with environmental degrees of freedom[48,49]. While the technique was originally introduced to study decoherence effects in mesoscopic devices, it was recently applied to explore electronic conduction in organic and biological molecular junctions[50–53], as well as anharmonic effects in (purely) phononic quantum conduction[54–56]. Particularly, in Ref.[57] we demonstrated that the LBP method can capture different transport regimes in molecular wires: tunneling conduction, ballistic motion, and incoherent hopping. In Refs.[58,59], we further used the LBP technique to simulate high-bias voltage effects, specifically the role of environmental interactions on the diode operation. More recently, we demonstrated that the LBP method can uncover an intermediate quantum coherent-incoherent transport regime in DNA junctions[60].

In this work, our objective is to study the thermoelectric effect in molecular junctions in situations when different transport mechanisms play a role: superexchange, phase coherent ballistic motion, and multi-step hopping. We perform our simulations using two variants of the probe technique: voltage probe (VP), which hands over the electrical conductance, and voltage-temperature probe (VTP), which generalizes the VP method by including both voltage and temperature biases, allowing us to simulate the thermopower of a junction[61–64]. Our specific objectives are: (i) Develop analytic expressions for the thermopower in molecular junctions covering different transport regimes (superexchange, ballistic tunneling, hopping). (ii) Understand the transition between the different mechanisms based on numerical simulations. (iii) Use simulations to explore the recently reported tunneling-to-hooping crossover in DNA molecules as manifested in the thermopower[12].

Below we illustrate that the three transport regimes can be identified based on the combined length and temperature dependence of G and S. However, while G can be suppressed by orders of magnitude as we increase molecular length, changes in S are rather modest over the whole range. Another interesting observation concerns the temperature dependence of the thermopower, which is identical (linear) in the tunneling and hopping regimes, while in the ballistic regime we find that $S \propto 1/T$. Finally, our LBP simulations of charge transport in DNA molecules reproduce the tunneling-to-hopping turnover in qualitative agreement with measurements[12]—once we suppress ballistic current.

The paper is organized as follows. In Sec. II, we

present the voltage-temperature probe technique. In Sec. III, we introduce a simple 1-dimensional (1D) model for charge conduction in linear molecules, develop analytic expressions for the thermopower in different regimes, and support these expressions with numerical simulations. Simulations of double-stranded DNA junctions with A:T blocks forming tunneling barriers are included in Sec. IV. We conclude in Sec. V.

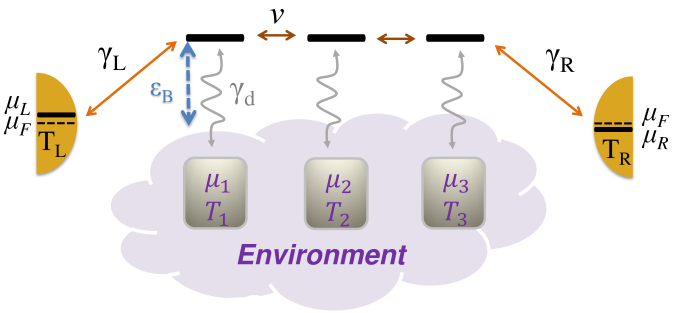

FIG. 1. Scheme of the 1D molecular junction model examined in this work for $N = 3$. The conductance and the thermopower are calculated using the LBP method, mimicking environmental effects in the junction with probes. In the thermopower calculation, the inner reservoirs' chemical potentials and temperatures are self-consistently determined so as to satisfy zero charge and heat dissipation conditions. Full-line arrows depict tunneling events in the molecule. Curly arrows describe transitions between molecular states and the probes.

II. METHOD: VOLTAGE-TEMPERATURE PROBE

The LBP method introduces environmental effects including decoherence, energy exchange, and dissipation into charge transport calculations. To compute the electrical conductance, we use the voltage probe as implemented in Ref.[57]. To simulate a thermal gradient and compute the thermopower, however, we have also to self-consistently set the temperature of the thermal environment, which we compute via the voltage-temperature probe method[61,64]. We begin with a general presentation of the VTP technique.

The molecular structure is described by a tight-binding Hamiltonian with N sites. The Hamiltonian includes the static energies of the localized molecular orbitals and charge transfer integrals between molecular orbitals centered on different sites. Each molecular site is coupled to a probe reservoir $j = 1, 2, ...N$, which can exchange particles and energy with the molecular system. As well, we assume that the left and right end groups are coupled to physical reservoirs (electrodes) $\nu = L, R$, where we impose the boundary conditions: chemical potentials $\mu_{L,R}$ and temperature $T_{L,R}$. Below we use the index α to identify all leads: the two metal electrodes $\nu = L, R$ and the $j = 1, 2, .., N$ probes, acting on each site. The total-net charge current, leaving the L contact, is written as (per spin specie)

$$I_L = \frac{e}{\hbar}\sum_{\alpha}\int_{-\infty}^{\infty}\mathcal{T}_{L,\alpha}(\epsilon)\left[f_L(\epsilon) - f_\alpha(\epsilon)\right]d\epsilon. \tag{1}$$

Here, $f_\alpha(\epsilon) = [e^{\beta_\alpha(\epsilon-\mu_\alpha)}+1]^{-1}$ is the Fermi function in the electrodes, given in terms of the inverse temperature $k_B T_\alpha = \beta_\alpha^{-1}$ and chemical potentials μ_α, k_B is the Boltzmann constant. The probe parameters, μ_j and T_j, are determined from the voltage-temperature probe condition, to be explained below. The transmission functions in Eq. (1) are obtained from the $N \times N$-sized molecular Green's function and the hybridization matrices[15],

$$\mathcal{T}_{\alpha,\alpha'}(\epsilon) = \mathrm{Tr}[\hat{\Gamma}_\alpha(\epsilon)\hat{G}^r(\epsilon)\hat{\Gamma}_{\alpha'}(\epsilon)\hat{G}^a(\epsilon)]. \tag{2}$$

The trace is performed over the molecular states. The retarded Green's function is given by

$$\hat{G}^r(\epsilon) = [\hat{I}\epsilon - \hat{H}_M + i\hat{\Gamma}/2]^{-1}, \tag{3}$$

with $\hat{G}^a(\epsilon) = [\hat{G}^r(\epsilon)]^\dagger$, $\hat{\Gamma} = \hat{\Gamma}_L + \hat{\Gamma}_R + \sum_{j=1}^{N}\hat{\Gamma}_j$, and $\hat{H}_M$ the Hamiltonian of the N-state molecular system. In structures considered in this work, the molecule is coupled to each metal lead through a single site, with the left (right) lead coupled to site '1' ('N'). The L, R hybridization matrices therefore include a single nonzero value,

$$[\hat{\Gamma}_L]_{1,1} = \gamma_L, \quad [\hat{\Gamma}_R]_{N,N} = \gamma_R, \tag{4}$$

with $\gamma_{L,R}$ describing the metal-molecule coupling energy. We work in the wide-band limit: We take $\gamma_{L,R}$ as energy independent parameters and ignore energy shifts of electronic states due to the metal leads. The hybridization matrices $\hat{\Gamma}_j$ describe the coupling of the jth probe to the respective site. For simplicity, we assume that incoherent effects are local, uncorrelated, and uniform, with $\gamma_d/\hbar$ as the rate constant due to environmental processes,

$$[\hat{\Gamma}_j]_{j,j} = \gamma_d, \quad j = 1, 2, .., N \tag{5}$$

We now explain the voltage-temperature probe condition which we employ in the linear response regime. We set the chemical potentials and the temperatures at the boundaries (μ_L, T_L) and (μ_R, T_R). At finite coupling strength γ_d, conducting electrons can tunnel back and forth from the molecular system into the probes. To enforce charge conservation between source (L) and drain (R), the charge current leaking to each probe, I_j, is made to nullify. Heat leakage Q_j to the probes is also prohibited. These two conditions translate into $2 \times N$ equations for the probes' chemical potentials μ_j and temperatures T_j,

$$\begin{aligned} I_j &= \frac{e}{\hbar}\sum_{\alpha}\int_{-\infty}^{\infty} d\epsilon\mathcal{T}_{j,\alpha}(\epsilon)\left[f_j(\epsilon) - f_\alpha(\epsilon)\right] = 0 \\ Q_j &= \frac{1}{\hbar}\sum_{\alpha}\int_{-\infty}^{\infty} d\epsilon(\epsilon-\mu_j)\mathcal{T}_{j,\alpha}(\epsilon)\left[f_j(\epsilon) - f_\alpha(\epsilon)\right] = 0 \end{aligned} \tag{6}$$

In the linear response regime (small bias and small temperature difference), we Taylor-expand the Fermi function,

$$f_\alpha(\epsilon,T_\alpha,\mu_\alpha)=f_{eq}(\epsilon,T_{eq},\mu_{eq}) -\frac{\partial f_{eq}(\epsilon,T_{eq},\epsilon_F)}{\partial\epsilon}\left[\frac{\epsilon-\epsilon_F}{T_{eq}}(T_\alpha-T_{eq})+(\mu_\alpha-\epsilon_F)\right]. \quad (7)$$

We explicitly indicate the dependency of the Fermi function on the equilibrium temperature T_{eq} and the Fermi energy ϵ_F. For convenience, below we set $\epsilon_F=0$. The $2N$ equations in Eq. (6) can be organized as follows ($p=0,1$),

$$\sum_\alpha\int_{-\infty}^{\infty}d\epsilon\mathcal{T}_{j,\alpha}(\epsilon)\left(-\frac{\partial f_{eq}}{\partial\epsilon}\right)(\epsilon-\epsilon_F)^p\left[\frac{\epsilon-\epsilon_F}{T_{eq}}(T_j-T_\alpha)+(\mu_j-\mu_\alpha)\right]=0 \quad (8)$$

The N equations with $p=0$ ($p=1$) correspond to charge (heat)-current equations (6). We solve this linear system and obtain the probes' chemical potentials μ_j and temperatures T_j. In the next step, the set $\{\mu_j,\,T_j\}$ is used in the calculation of the net current flowing across the device. Eq. (1) provides the charge current leaving the L terminal, which (given the probe condition) is identical to the current arriving at the drain R. After linearizing this equation we receive

$$I_L=\frac{e}{h}\sum_\alpha\left[(\mu_L-\mu_\alpha)\int_{-\infty}^{\infty}\mathcal{T}_{L,\alpha}(\epsilon)\left(-\frac{\partial f_{eq}}{\partial\epsilon}\right)d\epsilon + (T_L-T_\alpha)\int_{-\infty}^{\infty}\mathcal{T}_{L,\alpha}(\epsilon)\left(-\frac{\partial f_{eq}}{\partial\epsilon}\right)\left(\frac{\epsilon-\epsilon_F}{T_{eq}}\right)d\epsilon\right]. \quad (9)$$

The thermopower, or the Seebeck coefficient, is defined as

$$S=-\frac{\Delta V}{\Delta T}\Big|_{I_L=0}, \quad (10)$$

with $\Delta\mu=e\Delta V=\mu_L-\mu_R$ and $\Delta T=T_L-T_R$. We organize Eq. (9) as $I_L=L_{1,1}e\Delta V+L_{1,2}k_B\Delta T$ and write the thermopower, in the language of the linear response coefficients as $S=\frac{k_B}{e}L_{1,2}/L_{1,1}$. To calculate the linear conductance of the junction we set $\Delta T=0$. We then work with the voltage probe method[57] and study—in the linear response regime—the resistance of the junction $R\equiv(\Delta V)/I_L$, or its conductance $G=R^{-1}$.

III. 1-DIMENSIONAL MODEL

In this Section we use a simple 1-dimensional (1D) model to derive approximate analytical results for S in different transport regimes. We then perform numerical simulations using the VP and the VTP methods and present the electrical conductance and the thermopower hand in hand. The tunneling-to-hopping transition is clearly exhibited in the electrical conductance as a crossover from an exponential decay to a weak, Ohmic-like, distance dependence. As we show below, the thermopower can also indicate on this transition.

A. Hamiltonian

We consider a simple tight-binding 1D model with nearest-neighbor electronic coupling v_a and a uniform on-site energy ϵ_B,

$$\hat{H}_M=\sum_{j=1}^{N}\epsilon_B\hat{c}_j^\dagger\hat{c}_j+\sum_{j=1}^{N-1}v_a\left(\hat{c}_j^\dagger\hat{c}_{j+1}+h.c.\right). \quad (11)$$

Eq. (11) serves as the molecular Hamiltonian $\hat{H}_M$ in Eq. (3). To capture the tunneling-to-hopping crossover we consider chains with $N=2-10$ sites with parameters satisfying $v_a/\epsilon_B\ll1$. Specifically, we select $\epsilon_B=0.5$ eV and $v_a=0.05$ eV. The metal-molecule hybridization $\gamma_{L,R}$ is taken in the range 0.05 - 0.5 eV. We work with a wide range of temperatures, $T_{eq}=5-300$ K, and play with environmental effects in the range $\gamma_d=0-0.2$ eV.

B. Analytic results

We derive here approximate analytical expressions for the thermopower in the three relevant transport limits, tunneling, ballistic, and hopping. We begin by explaining the behavior of the thermopower when environmental effects are ignored. Based on the Landauer Formula [Eq. (9) without probes], we receive

$$S=\left(\frac{1}{eT}\right)\frac{\int d\epsilon\mathcal{T}(\epsilon)\left(-\frac{\partial f_{eq}}{\partial\epsilon}\right)(\epsilon-\epsilon_F)}{\int d\epsilon\mathcal{T}(\epsilon)\left(-\frac{\partial f_{eq}}{\partial\epsilon}\right)}. \quad (12)$$

Here e is the charge of an electron (with a negative sign). We now evaluate this expression in two limits. First, in the deep tunneling regime, $|\epsilon_B-\epsilon_F|\gg v_a,\gamma_{L,R},k_BT$, we only need to consider the behavior of the transmission function at the vicinity of the Fermi energy. Since we are missing sharp features (resonances) in this region, we Taylor-expanded the transmission function as

$$\mathcal{T}(\epsilon)\sim\mathcal{T}(\epsilon_F)+\frac{\partial\mathcal{T}(\epsilon)}{\partial\epsilon}\Big|_{\epsilon_F}(\epsilon-\epsilon_F). \quad (13)$$

We plug this expansion into Eq. (12), and note that since the derivative of the Fermi function is approximately a

delta function around the Fermi energy at low temperatures, the first contribution vanishes, and we are left with the familiar behavior

$$S = \frac{1}{eT}\frac{\left.\frac{\partial \mathcal{T}(\epsilon)}{\partial \epsilon}\right|_{\epsilon_F}\int d\epsilon \left(-\frac{\partial f_{eq}}{\partial \epsilon}\right)(\epsilon-\epsilon_F)^2}{\mathcal{T}(\epsilon_F)\int d\epsilon \left(-\frac{\partial f_{eq}}{\partial \epsilon}\right)} = \frac{\pi^2 k_B^2 T}{3e}\left(\frac{\left.\frac{\partial \mathcal{T}(\epsilon)}{\partial \epsilon}\right|_{\epsilon_F}}{\mathcal{T}(\epsilon_F)}\right). \quad (14)$$

Note that e is the charge of an electron. With this sign convention, this expression agrees with other studies, see e.g.[3,6,9–11]. We can in particular explore the superexchange limit. In this (tunneling, T) case, the transmission function decays exponentially with length[15],

$$\mathcal{T}_T(\epsilon) = \left(\frac{v_a}{\epsilon-\epsilon_B}\right)^{2N}\frac{\gamma_L\gamma_R}{v_a^2}, \quad (15)$$

resulting in the conductance $G_T = G_0\mathcal{T}_T(\epsilon_F)$, G_0 is the quantum of conductance. Using Eq. (15) in (14), we receive what we refer to as the 'tunneling-superexchange' thermopower,

$$S_T = \frac{\pi^2}{3}\left(\frac{k_B}{e}\right)\frac{k_BT}{\epsilon_B-\epsilon_F}\times 2N. \quad (16)$$

This expression predicts the following properties—which were verified in experiments[7,8,10]: In the deep tunneling regime, the thermopower increases linearly with temperature and with the number of molecular sites N. As well, LUMO conduction, with ϵ_B situated above the Fermi energy, shows a negative thermopower.

We now consider the coherent on-resonant (ballistic, B) case. In the limit of weak metal-molecule hybridization, the transmission displays sharp features which we approximate by a Dirac delta function, $\mathcal{T}_B(\epsilon) \sim A\delta(\epsilon-\epsilon_B)$, A is a parameter with the dimension of energy. Using Eq. (12), we find that ballistic electrons organize the thermopower

$$S_B = \left(\frac{k_B}{e}\right)\left(\frac{\epsilon_B-\epsilon_F}{k_BT}\right). \quad (17)$$

Interestingly, in the coherent-resonant regime the scaling of the thermopower with temperature and with bridge height ϵ_B are opposite to trends observed in the deep tunneling limit.

We now examine situations suffering from environmental effects, $\gamma_d \neq 0$. In this case, the conductance manifests hopping (Ohmic) conduction for long enough molecules. In the language of the probe technique, we recall that at low temperatures we can organize an expression for the thermopower in the form of Eq. (12), with an *effective* transmission function which comprises the contributions of the probes[65]. We can Taylor expand this effective (probe dependent) transmission function and organize the result in the structure of Eq. (14). What is the form of this probe dependent transmission function in the hopping (H) regime, $\mathcal{T}_H(\epsilon)$? Based on simulations, in Ref.[57] we proposed the following structure:

$$\mathcal{T}_H(\epsilon) \sim \frac{\gamma_d^2 v_a^2}{(\epsilon_B-\epsilon)^4 f(N)}, \quad (18)$$

with the conductance $G_H \sim G_0\mathcal{T}_H(\epsilon)$. The function $f(N)$ depends on the molecular length N, approximately in a linear manner. Substituting Eq. (18) into Eq. (14), we arrive at a rather simple approximation for the thermopower, valid in the hopping regime,

$$S_H \sim \left(\frac{k_B}{e}\right)\frac{4\pi^2}{3}\frac{k_BT}{(\epsilon_B-\epsilon_F)}. \quad (19)$$

Surprisingly, this expression is almost identical to the superexchange limit, Eq. (16)—only replacing the linear dependency on $2N$ with a factor 4. Recall that Eq. (19) was organized based on the D'Amato Pastawski effective transmission formula[65], which is limited in applicability to the low temperature regime and to off-resonance situations. Our numerical simulations below did not rely on this approximation, though we note that since selected parameters satisfy $|\epsilon_B-\epsilon_F| \gg v_a, k_BT$, we are essentially considering low-temperature situations.

Equation (19) is rather interesting. It predicts that when the current is dominated by hopping conduction, the thermopower reaches a constant value, independent of molecular length and environmental interactions γ_d. Furthermore, this expression predicts that $S_H \sim S_T(N=2)$. As a result, another concrete expectation is that at low temperatures $\epsilon_B \gg v_a, k_BT$, $S(N)$ should be a concave function, since the hopping thermopower lies below the coherent value. Both of these predictions agree with measurements of DNA molecules[12].

Note that in Ref.[47], the hopping conduction was argued to follow Eq. (17), identical to the ballistic behavior. We point out that Eq. (25) of Ref.[47] was incorrectly attributed to hopping behavior, and in fact it corresponds as well to ballistic motion. Thus, to the best of our knowledge, Eq. (19) here is the first analytical construction for the thermopower in the hopping transport regime.

C. Simulations

We study the coherent limit ($\gamma_d = 0$) in Fig. 2. To identify the tunneling-to-ballistic transition, we follow both the electrical conductance and the thermopower. In the off-resonance tunneling regime (low temperature and short junctions), the conductance decays exponentially with length. At the same time, the thermopower grows linearly with N, with a slope in precise agreement with Eq. (16). At high temperatures and for long enough chains, the ballistic regime dominates and both the conductance and the thermopower become independent of length, with Eq. (17) very accurately predicting the asymptotic value for S. Specifically, we immediately

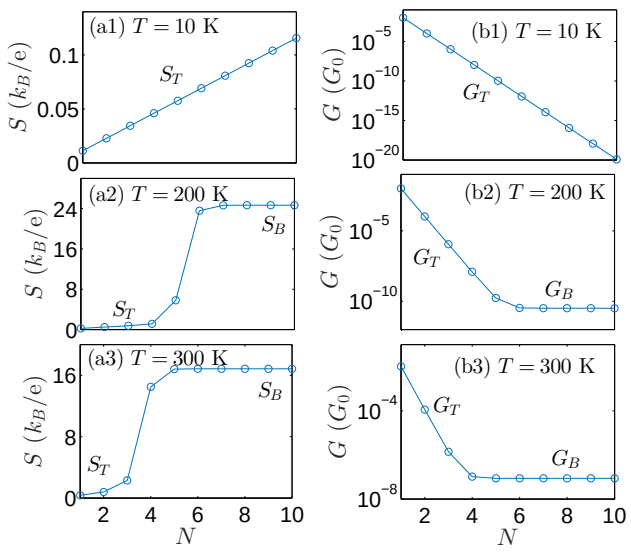

FIG. 2. Coherent transport in the 1D Model. (a1-a3) Thermopower and (b1-b3) electrical conductance as a function of molecular length at temperatures (a1,b1) 10 K, (a2,b2) 200 K and (a3,b3) 300 K. We use $\epsilon_B = 0.5$, $v_a = 0.05$, $\gamma_{L,R} = 0.05$, all in eV. The different limits, deep tunneling and ballistic motion, are labeled.

confirm that in the ballistic regime S scales with T^{-1}, in a sharp contrast to the off-resonant tunnelling behavior, supporting $S \propto T$.

Figure 3 illustrates the result of incoherent effects on S, using γ_d=1, 10, 100 meV. A tunneling-to-hopping crossover is observed in both conductance and thermopower if the system is maintained at relatively low temperatures and γ_d is made large enough to support hopping transport. Specifically, in panel (a1), we use $T = 100$ K. S then grows linearly for short N and saturates to the hopping value $S \sim 0.25\ k_B/e$, independent of N and γ_d. This number excellently agrees with the prediction of Eq. (19). At high temperatures (room temperature in our case), the tail of the Fermi function enhances the ballistic contribution—even beyond hopping conduction[57]. Indeed, in panel (a2) with T =200 K we observe that the ballistic component is enhanced over the hopping contribution at small γ_d. Finally, in panel (a3) we clearly see that at room temperature, the thermopower at $\gamma_d = 1$ meV follows a ballistic trend, while at $\gamma_d = 100$ meV it displays hopping characteristics. Simultaneously, we confirm that the electrical conductance displays corresponding transitions between different mechanisms: exponential decay with length for short chains, length independence when γ_d is small and the chain is long (ballistic conduction), and an Ohmic behavior, $G_H \propto 1/N$, for large γ_d in long enough chains.

Activated conduction takes place in both ballistic and hopping regimes. Therefore, identifying an Arrhenius factor in the conductance does not conclusively identify thermally activated incoherent hopping processes[17,18]. This aspect is demonstrated in Fig. 4(a), with the conductance showing a typical crossover from an activationless to an activated form as we increase the temperature, even when environmental effects are turned off completely with $\gamma_d = 0$, see also Ref.[57]. Temperature-dependent conductance measurements can thus be quite confusing to interpret. In contrast, the temperature dependence of the thermopower clearly separates ballistic and hopping contributions: $S \propto T$ in both the deep tunneling and the hopping regimes, but $S \propto 1/T$, when electrons ballistically cross the junction, see Fig. 4. We particularly emphasize (panel c) that around room temperature hopping is the dominant transport mechanism, when $\gamma_d \sim 100$ meV. We also note that at low temperatures S is always linear; the slope corresponds to the molecular length in the deep tunneling regime, when Eq. (16) is satisfied.

In Fig. 5 we turn our attention to junctions with a low energy barrier, $\epsilon_B \sim v_a$, k_BT. In this limit, the conductance *decreases* with increasing γ_d (squares), as opposed to the case with $|\epsilon_B/v_a| \gg 1$ (circles). We observe that the thermopower weakly depends on distance when $|\epsilon_B/v_a| \sim 1$, and that its magnitude is reduced with γ_d. These effects both come about because as we increase γ_d we broaden molecular resonances, resulting in dampening of on-resonance conduction, and flattening the transmission function, the derivative of which roughly dictates S.

We now comment on the sign of the thermopower in our simulations. Calculations in this Section assumed electron transport. The factor k_B/e should be evaluated with the negative sign for the unit of charge, to receive negative values for S in Figs. 2-5. Since our 1D model concerns LUMO transport, negative value for S conforms with the literature[2].

IV. TUNNELING TO HOPPING TRANSITION IN DNA

In the previous section we demonstrated that the thermopower exhibits signatures of underlying transport mechanisms. Particularly, panel (a1) of Fig. 3 manifests the characteristic tunneling-to-hopping crossover. This result qualitatively captures recent experimental reports over a related behavior in DNA molecules[12]. While in Sec. III we employed a simple 1D tight-binding model to describe generic molecular chains, our objective in this section is to use a more detailed model Hamiltonian for simulating charge transport in double-stranded (ds) DNA structures. Particularly, we consider here G:C rich sequences with an inserted A:T block, as well as alternating GC sequences. See Table I for the list of sequences examined. We compute simultaneously the conductance and thermopower in these molecules, with an effort to reproduce and explain recent measurements[12]. Our analysis further furnishes us with a better understanding of the limitations of the LBP method in simulating biomolecules.

Simulating charge transport in DNA molecules is an

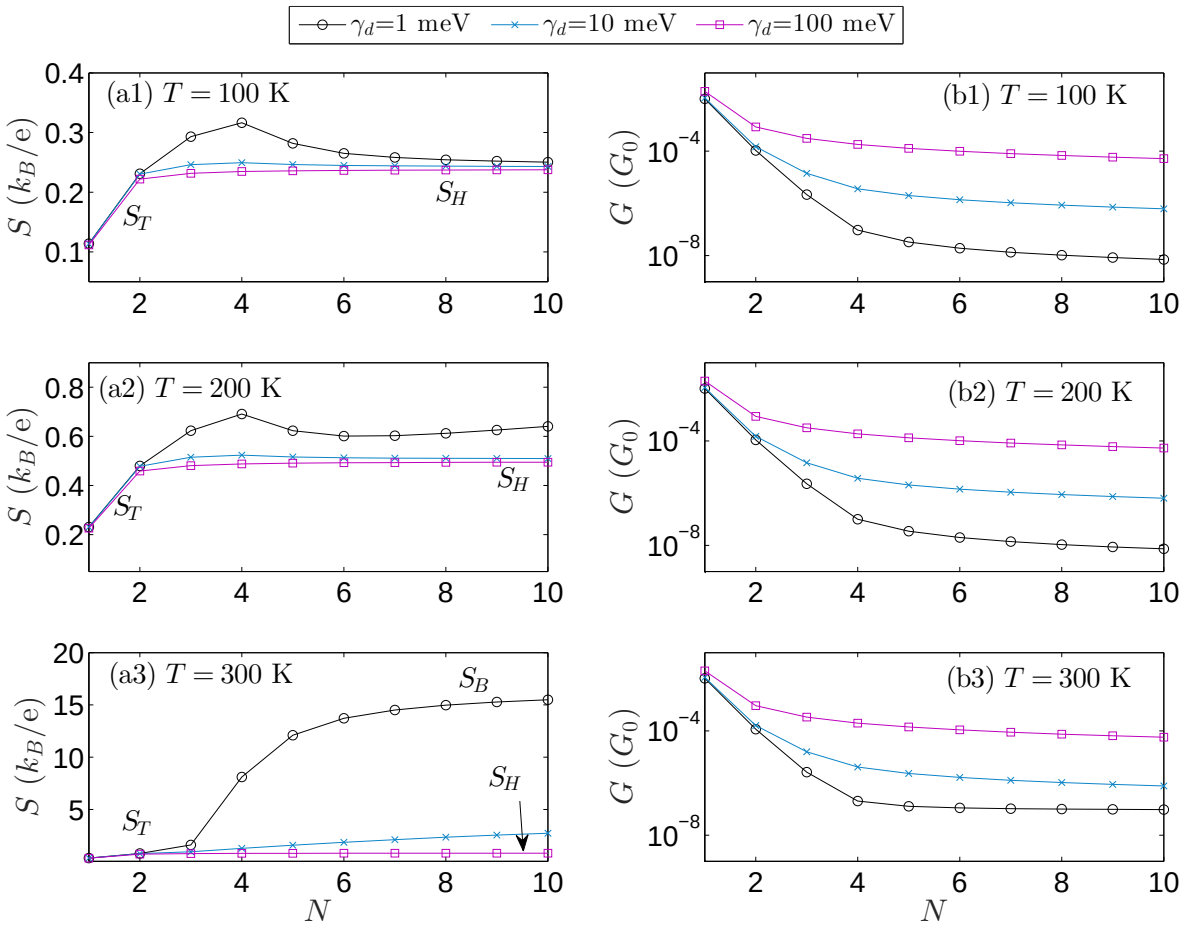

FIG. 3. 1D Model with environmental effects. (a1-a3) Thermopower and (b1-b3) conductance as a function of molecular length for the temperatures 100 K, 200 K and 300 K, with γ_d=1, 10, 100 meV, as indicated in the panels. Other parameters are $\epsilon_B = 0.5$, $v_a = 0.05$, $\gamma_{L,R} = 0.05$, in eV. The different limits for S, deep tunneling, ballistic motion, and hopping conduction, are marked.

exceptionally challenging task given their complex electronic structure and with rich structural, solvent and counterion dynamics. Among the approaches devised to follow charge transport in these systems we recount here kinetic rate equations[66–68], which capture hopping transport, and the Landauer approach, which describes only the coherent limit[69], see a recent application in Ref.[70]. Simulating intermediate coherent dynamics in DNA is an intricate task: This regime can be followed with phenomenological tools[60,71–73], or by combining classical molecular dynamics simulations (for describing the effect of backbone, solvent, counterions, and he DNA internal structural fluctuations) with quantum mechanics/molecular mechanics methodologies[74–78]. Alternatively, in Ref.[79] charge transport in DNA was simulated using a stochastic Schrödinger equation while taking into account temporal and spatial fluctuations in electronic parameters. In other methods, one explicitly includes the interaction of transport charges with selected DNA vibrational modes using e.g. Green's function approaches[80], quantum rate equations[81], or semiclassical approximations[82].

Our simulations here are based on the LBP method as explained in Sec. II. In a recent application of this technique to DNA[60], we demonstrated that the LBP method can yield results in qualitative (and sometimes quantitative) agreement with experiments, and uncovered an intermediate coherent-incoherent transport regime[83]. An important caveat of our simulations is the fact that ballistic transport is promoted beyond what we expect in reality, since the underlying electronic structure used is static. To overcome this deficiency, and limit the ballistic conduction, in our simulations below we have reduced the temperature while keeping environmental effects active with a finite γ_d of 5-50 meV. This modification allows us to nicely recover experimental trends for both the electrical conductance and the thermopower, see Figs. 7-8. Note that in our simulations the parameter γ_d, which controls the rate of electron scattering with environmental degrees of freedom, is independent from the temper-

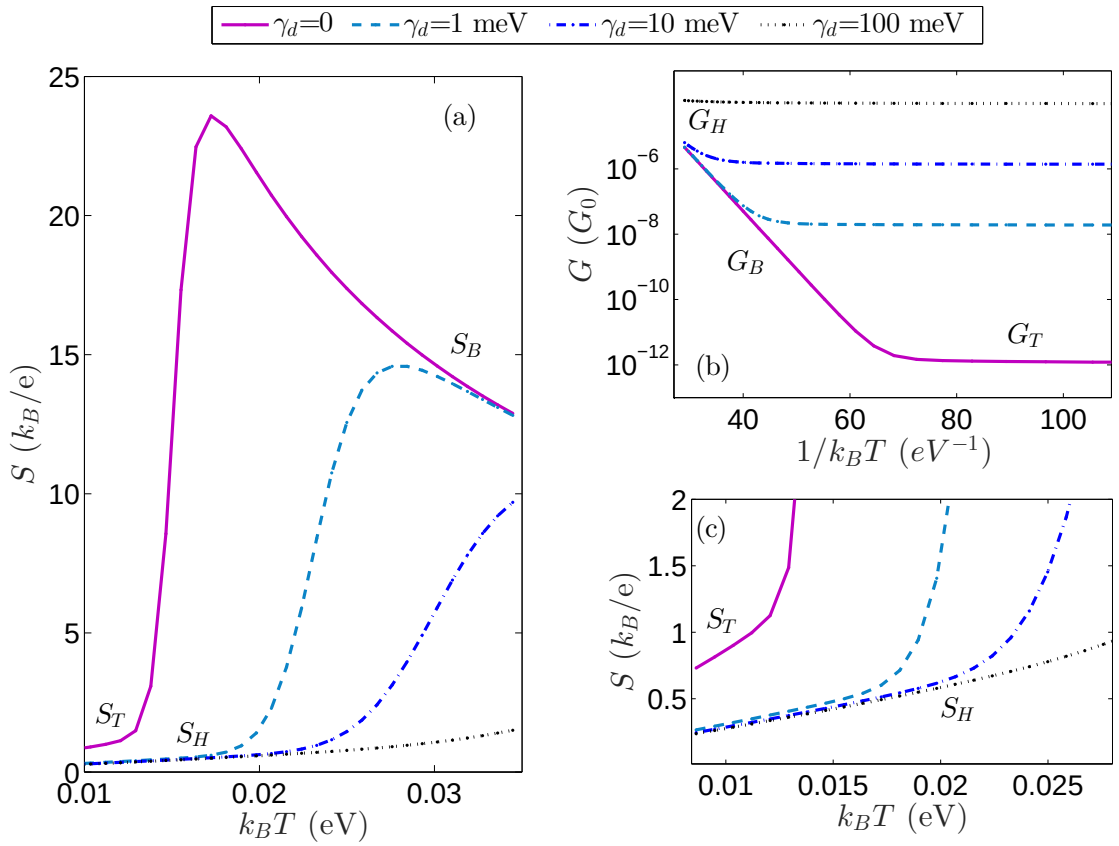

FIG. 4. (a) Thermopower and (b) electrical conductance as a function of temperature in the 1D model with $N = 6$ sites, $\gamma_d = 0, 1, 10, 100$ meV. Panel (c) zooms over S in the range 100 - 330 K. Other parameters are $\epsilon_B = 0.5$, $v_a = 0.05$, $\gamma_{L,R} = 0.05$ all in eV. We identify by $G_{T,B,H}$ and $S_{T,B,H}$ the limiting behavior of off-resonance tunneling, on-resonance ballistic, and hopping conduction.

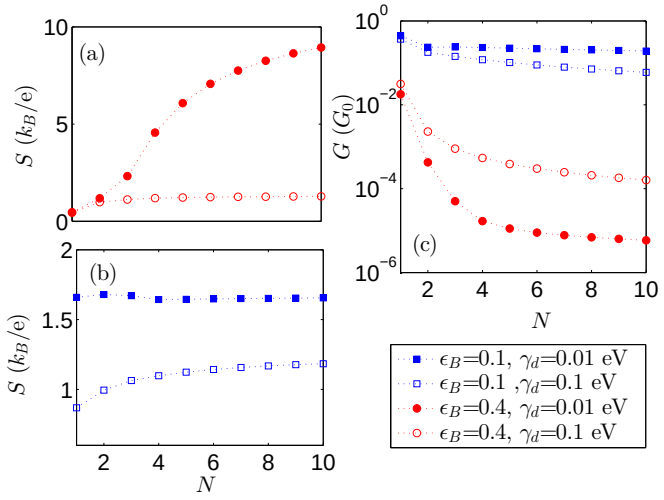

FIG. 5. 1D model in the limits $\epsilon_B \gg v_a$ (○) and $\epsilon_B \sim v_a$ (□). (a)-(b) Thermopower and (c) electrical conductance as a function of number of sites at room temperature, $T = 300$ K. Other parameters are $v_a = 0.05$, $\gamma_{L,R} = 0.05$ all in eV.

ature. The single role of the temperature is therefore to broaden the Fermi functions, thus directly controlling the injection of ballistic charges at the tail of the Fermi function.

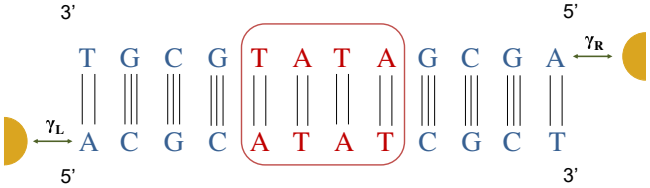

FIG. 6. Example for a 12-base pair DNA duplex simulated in this work, ACGC(AT)$_2$GCGT. The AT barrier is highlighted by the box.

Table I: **Sequences studied in this work, with measurements reported in Ref.[12].**

number of base pairs (molecular length)	5'-A$(CG)_m$T-3' $m=3-8$	5'-ACGC$(AT)_m$GCGT-3' and 5'-ACGC$(AT)_{m-1}$AGCGT-3', $m=1-4$
8	A$(CG)_3$T	
9		ACGCAGCGT
10	A$(CG)_4$T	ACGCATGCGT
11		ACGCATAGCGT
12	A$(CG)_5$T	ACGC$(AT)_2$GCGT
13		ACGC$(AT)_2$AGCGT
14	A$(CG)_6$T	ACGC$(AT)_3$GCGT
15		ACGC$(AT)_3$AGCGT
16	A$(CG)_7$T	ACGC$(AT)_4$GCGT
18	A$(CG)_8$T	

A. Model

We model charge transport in DNA using a tight-binding ladder model Hamiltonian, see e.g. Refs.[71,80,84–86]. This Hamiltonian describes the topology of a ds-DNA molecule which is n base-pairs long, with each site representing a particular base; $N=2n$ is the total number of bases. We assume that charge transport takes place along the base-pair stacking and we ignore the backbone,

$$\hat{H}_M=\sum_{j=1}^{n}\Bigg[\sum_{s=1,2}\epsilon_{j,s}\hat{c}^{\dagger}_{j,s}\hat{c}_{j,s}+\sum_{s\neq s'=1,2}t_{j,ss'}\hat{c}^{\dagger}_{j,s}\hat{c}_{j,s'} + \sum_{s,s'=1,2}t_{j,j+1,ss'}(\hat{c}^{\dagger}_{j,s}\hat{c}_{j+1,s'}+h.c.)\Bigg]. \quad (20)$$

The index $s=1,2$ identifies the strand. $\hat{c}^{\dagger}_{j,s}$ creates a hole on strand s at the jth site with an on-site energy $\epsilon_{j,s}$. $t_{j,ss'}$ and $t_{j,j+1,ss'}$ are the electronic matrix elements between nearest neighboring bases. This model mimics the topology of the ds-DNA molecule; helical effects are taken into account within renormalized electronic parameters.

We use the parametrization of Ref.[87], distinguishing between backbone orientations (5' and 3'). In this parametrization, on-site energies depend on the identity of neighboring bases. Here, following Ref.[71], we simplify this description and assign a single value (averaged) for on-site energies for each base, see Table II. Electronic matrix elements were taken directly from Ref.[87].

We connect the DNA molecule to metal leads as sketched in Fig. 6, oriented so as to correspond to experiment[12]. Environmental effects (structural motion, solvent, counterions) are captured by the probes' condition implementing phase loss and inelastic effects.

Beyond the molecular electronic structure of the ds-DNA, three additional parameters should be provided as input to LBP equations: The position of the Fermi energy ϵ_F relative to the molecular states, the metal-molecule hybridization energy $\gamma_{L,R}$, and the electron-environment interaction energy, encapsulated within the parameter γ_d. In principle, we could use a range of values for γ_d to capture the susceptibility of different bases and sites along the DNA to environmental interactions. Here, for simplicity, we use a single value γ_d, identical for all bases and sites. Furthermore, we note that while one could carefully optimize these three parameters, ϵ_F, $\gamma_{L,R}$ and γ_d, to optimally reproduce experimental results, our goal here has been to reach a general understanding over the behavior of the thermopower under different mechanisms. Therefore, we present our results with representative parameters, reasonable for a junction geometry.

We now point out that by convention, our transport expressions are all written for electrons: We use the Fermi function $f(\epsilon)$ in the Landauer formula, standing for the occupation factor of electrons. However, the DNA parametrization which we use concerns holes[87]. While the conductance is unaffected by the identify of the charge carriers (it scales with e^2), this fact was taken into account in the evaluation of the thermopower, in physical units, as presented in Figs. 7-9. Note that in simulations presented below, the conductance was calculated including both spin species, using $G_0=2e^2/h$.

Table II: Selected on-site energies and inter-strand electronic coupling (eV). (See[87] for full parameter set.)

ϵ_G	ϵ_A	ϵ_C	ϵ_T	$t_{\mathrm{G\|\|C}}$	$t_{\mathrm{A\|\|T}}$
8.178	8.631	9.722	9.464	-0.055	-0.047

B. Results

The Seebeck coefficient and the resistance of DNA sequences with an AT block are included in Fig. 7, manifesting a clear tunneling-to-hopping transition around 11 base pairs. The tunneling behavior is characterized by an exponential enhancement of resistance and by a linear increase of the thermopower. The hopping regime shows an Ohmic resistance, and a marginal (yet nonzero) thermopower, below the coherent value. These qualitative trends are in an excellent agreement with the experiment[12]. Our simulations were performed at low

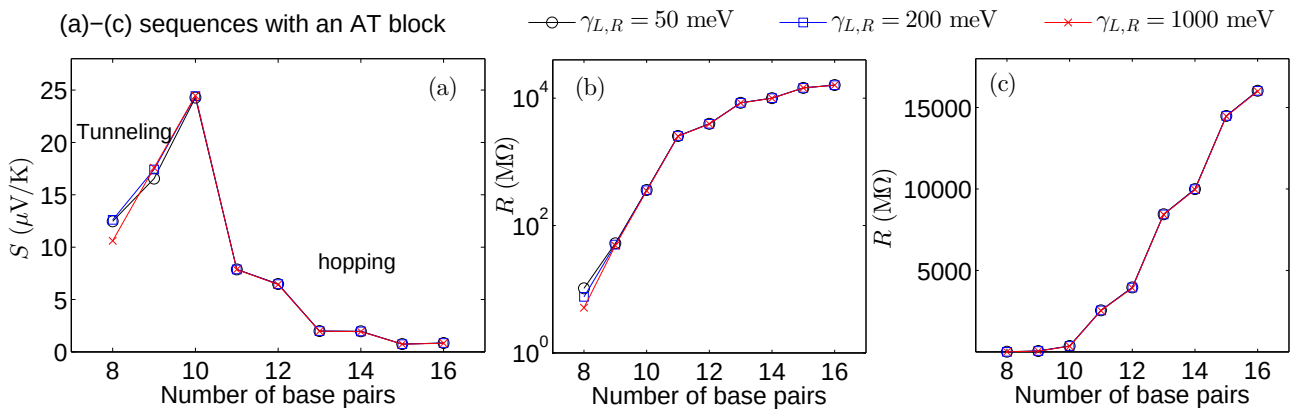

FIG. 7. (a) Thermopower and (b)-(c) electrical resistance in logarithmic and linear scale of DNA sequences with an AT block, ACGC(AT)$_m$GCGT and ACGC(AT)$_{m-1}$AGCG ($m = 1 - 4$), see Table I. Simulations were performed at T=5 K to attenuate the contribution of ballistic electrons. Other parameters are $\gamma_d = 10$ meV, $\gamma_{L,R}$=50, 200, and 1000 meV. The Fermi energy is placed at the energy of the G base, $\epsilon_F = \epsilon_G$.

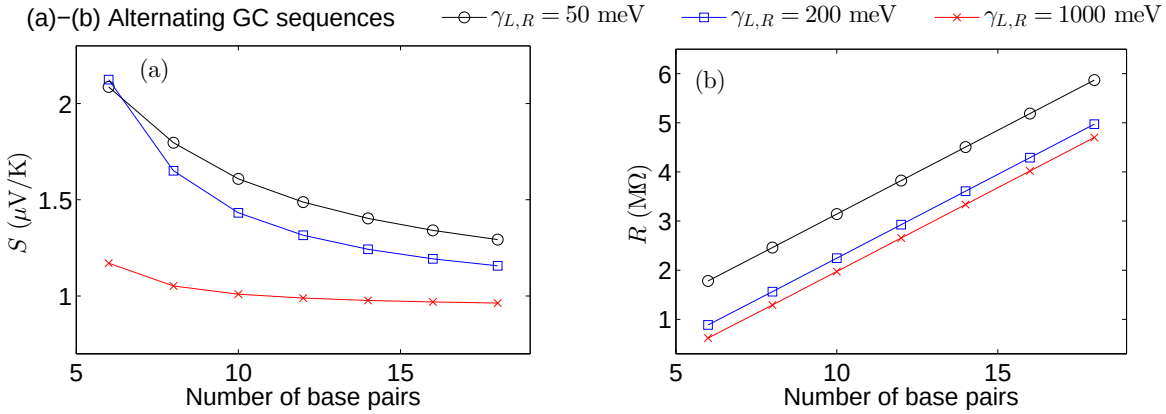

FIG. 8. (a) Thermopower and (b) electrical resistance of A(CG)$_m$T sequences, see Table I. Simulations were performed at T=5 K, $\gamma_d = 50$ meV, $\epsilon_F = \epsilon_G$.

temperatures to cut down on ballistic electrons which contribute beyond what is expected in reality, where static and dynamic disorder naturally reduce ballistic conduction. We further confirmed that our results only weakly depend on the metal-molecule hybridization energy. Note that we were not able to reproduce measurements in a quantitative manner, neither for the resistance, nor for the thermopower.

We recall that our expressions for linear chains predict that $S_T/(2n) = S_H/4$, see Eqs. (16) and (19); in the ds-DNA the number of base pairs n corresponds to the length. We examine the reported results of Ref.[12]: The tunneling value is $S_T(n = 10) = 6$ μV/K, while $S_H(n = 16) = 2$ μV/K. The ratio between these values reasonably satisfy theoretical predictions.

The Seebeck coefficient and the resistance of DNA sequences with alternating GC base-pairs (see Table I) are displayed in Fig. 8. Here, as confirmed in Ref.[60], the resistance increases linearly with length throughout, in accord with a multi-state hopping conduction mechanism. The thermopower shows monotonic behavior, continuously decreasing with length. We emphasize that (19) is invalid in the present conditions, as it was derived assuming high energy barriers relative to temperature These simulations were also performed at $T = 5$ K, as explained above. We adopted here the value $\gamma_d = 50$ meV, to reproduce experimental values for resistance. It should be noted however, as we show in Fig. 10, that our results for this family of sequences are quite robust in the range $\gamma_d = 5 - 100$ meV.

To establish our observations, in Figs. 9-10 we comprehensively test the behavior of the DNA junctions at different temperatures and values of γ_d. We do not display results with different values of the Fermi energy, as we observed that varying it by ± 0.1 eV lead to a significant increase of the resistance, further away from experimental values. Fig. 9 demonstrates that in sequences with an A:T barrier, the tunneling and hopping regimes are es-

tablished when the temperature is rather low $T = 5-100$ K and $\gamma_d = 5 - 20$ meV. Recall that we perform here low-temperature simulations so as to limit the injection of ballistic electrons, which are suppressed in real systems by dynamics and static fluctuations. Fig. 10(a1) specifically shows that at 100 K, S grows due to ballistic conduction. It is important to note that at the same time, the resistance does not well evince on the ballistic contribution (see panel b1) as it is over-dominated by the Ohmic behavior.

Our simulations indicate that a simultaneous examination of the electrical conductance and the thermopower is highly beneficial for correctly identifying transport mechanisms. In some situations, the resistance shows a linear enhancement, indicating on hopping conduction, yet at the same time the thermopower pinpoints on a significant contribution of on-resonance electrons. Regarding the experiment reported in Ref.[12], our VTP simulations support the identification of the different transport limits. We also suggest measuring the temperature dependence of G and S, around room temperature, for this family of DNA sequences (Table I). Establishing the relationship $S \propto T$ in both short and long sequences would further support the claim of hopping-dominated conduction in long duplexes.

V. SUMMARY

We developed analytical expressions for the thermopower of single molecule junctions, covering three different transport regimes: (i) off resonant (superexchange) and (ii) on-resonant (ballistic) tunneling, as well as (iii) multi-step hopping. Using the Landauer-Büttiker probe technique, we simulated the conductance and thermopower of 1D chains and conclusively identified transport mechanisms with varying temperature and molecular length. While the distance dependence of the thermopower can separate tunneling behavior from longer-range ballistic and hopping mechanisms, the temperature dependence is necessary to conclusively distinguish between these two, which are both largely distance independent.

We applied the probe approach to simulate the resistance and thermopower in two families of DNA molecules: sequences with an AT barrier which display a tunneling-to-hopping crossover with increasing barrier length, and alternating GC sequences, supporting hopping transport. Our LBP simulations qualitatively agree with recent measurements[12], providing a critical theoretical affirmation of these results. Specifically, we were able to reproduce the tunneling-to-hopping crossover close to the correct position.

Simulations of DNA structures were performed at rather low temperature to minimize the contribution of ballistic electrons (while keeping environmental effects with a finite value for γ_d). In reality, ballistic charge conduction is inhibited in DNA given its complex electronic structure and rich nuclear motion. Future work will incorporate energetic disorder with the aim of mimicking these rich dynamics, and naturally attenuating on-resonance coherent conduction.

This study complements our recent work on the LBP method, demonstrating its adequacy for simulating transport phenomena in single molecule junctions[57–60]. A concrete comparison between LBP simulations and other techniques, where many-body electron-phonon effects are explicitly included, is still missing, and will be the focus of future work.

ACKNOWLEDGMENTS

The work was supported by the Natural Sciences and Engineering Research Council of Canada and the Canada Research Chair Program. The work of Michael Kilgour was partially funded by an Ontario Graduate Scholarship. Roman Korol was partially funded by the University of Toronto Excellence Research Fund.

[1] J. A. Malen, S. K. Yee, A. Majumdar, and R. A. Segalman, Chem. Phys. Lett. **491**, 109 (2010).
[2] L. Rincon-Gracia, C. Evangeli, G. Rubio-Bollinger, and N. Agrait, Chem. Soc. Rev. **45**, 4285 (2016).
[3] P. Reddy, S.-Y. Jang, R. A. Segalman, and A. Majumdar, Science **315**, 1568 (2007).
[4] J. A. Malen, P. Doak, K. Baheti, T. D. Tilley, R. A. Segalman, and A. Majumdar, Nano Lett. **9**, 1164 (2009).
[5] K. Baheti, J. A. Malen, P. Doak, P. Reddy, S.-Y. Jang, T. D. Tilley, A. Majumdar, and R. A. Segalman, Nano Lett. **8**, 715 (2008).
[6] A. Tan, J. Balachandran, B. D. Dunietz, S.-Y. Jang, V. Gavini, and P. Reddy, Appl. Phys. Lett. **101**, 243107 (2012).
[7] J. R. Widawsky, P. Darancet, J. B. Neaton, and L. Venkataraman, Nano Lett. **12**, 354 (2012).
[8] J. R. Widawsky, W. Chen, H. Vazquez, T. Kim, R. Breslow, M. S. Hybertsen, and L. Venkataraman, Nano Lett. **13**, 2889 (2013).
[9] Y. Kim, W. Jeong, K. Kim, W. Lee, and P. Reddy, Nature Nanotechnol. **9**, 881 (2014).
[10] Y. Kim, A. Lenert, E. Meyhofer, and P. Reddy, Appl. Phys. Lett. **109**, 033102 (2016).
[11] S. Guo, G. Zhou, and N. Tao, Nano Lett. **13**, 4326 (2013).
[12] Y. Li, L. Xiang, J. Palma, Y. Asai, and N. Tao, Nature Comm. **7**, 11294 (2016).
[13] G. D. Mahan and J. O. Sofo, Proc. Nat. Acad. Sci. **93**, 7436 (1996).
[14] G. Benenti, G. Casati, K. Saito, and R. S. Whitney, arXiv:1608.05595.
[15] A. Nitzan, *Chemical Dynamics in Condensed Phases: Relaxation, Transfer, and Reactions in Condensed Molecular Systems;*, (Oxford University Press: Oxford, UK, 2006).
[16] J. C. Cuevas and Scheer, *Molecular Electronics: An Introduction to Theory and Experiment*, (World Scientific Publishing Company, Singapore, 2010).
[17] M. Poot, E. Osorio, K. O'Neill, J. M. Thijssen, D. Vanmaekelbergh, and C. A. van Walree, Nano Lett. **6**, 1031 (2006).
[18] G. Sedghi, V. M. Garcia-Suarez, L. J. Esdaile, H. L. Anderson, C. J. Lambert, S. Martin, D. Bethell, S. J. Higgins, M. Elliott, N. Bennett, J. E. Macdonald, and R. J. Nichols, Nature Nanotechnol. **6**, 517 (2011).
[19] S. H. Choi, B. Kim, and C. D. Frisbie, Science **320**, 1482 (2008).
[20] S. H. Choi, C. Risko, M. C. R. Delgado, B. Kim, J.-L. Bredas, and C. D. Frisbie, J. Am. Chem. Soc. **132**, 4358 (2010).
[21] J. C. Genereux and J. K. Barton, Chem. Rev. **110**, 1642 (2009).

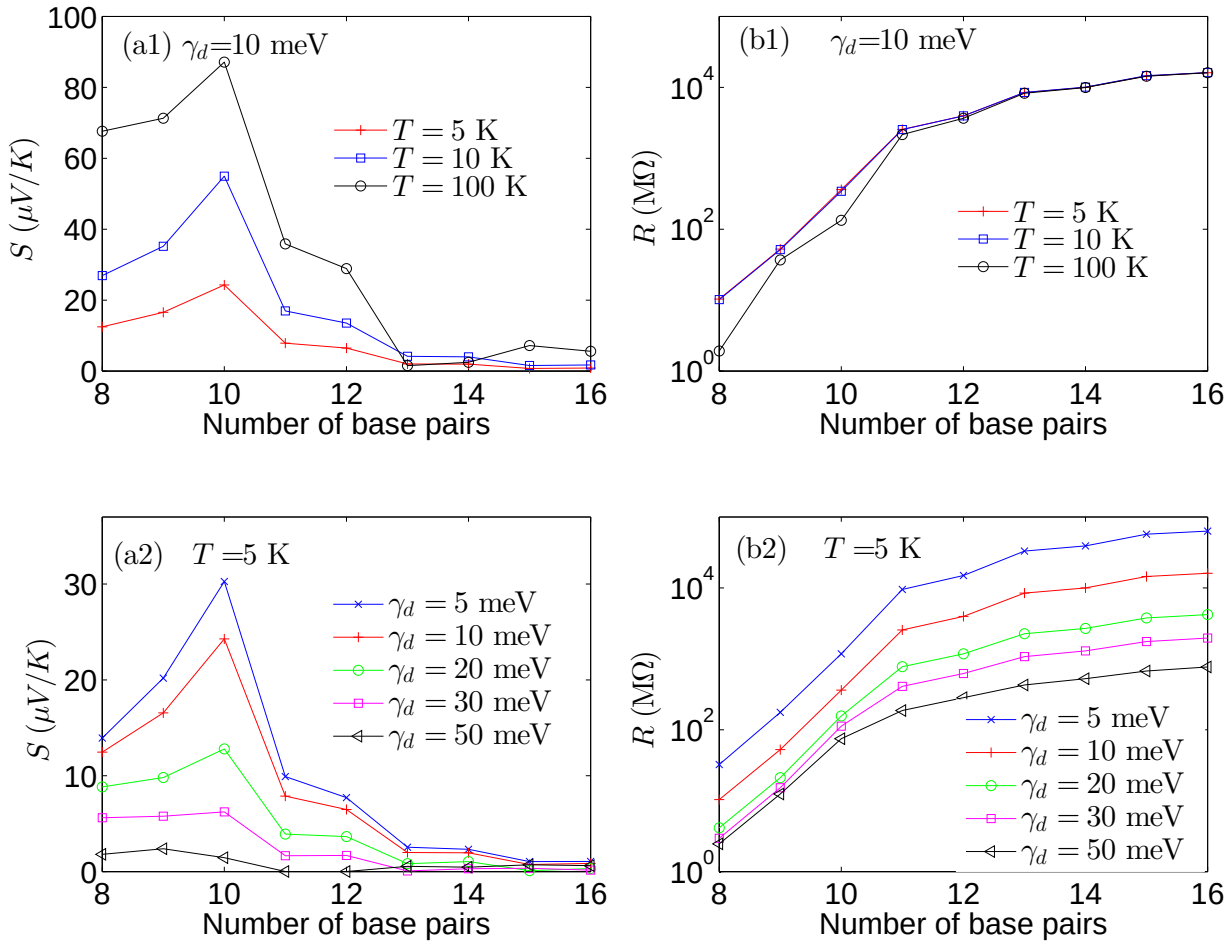

FIG. 9. (a) Thermopower and (b) electrical resistance of DNA sequences with an AT block, ACGC(AT)$_m$GCGT and ACGC(AT)$_{m-1}$AGCG ($m = 1 - 4$), see Table I, for a range of temperatures and environmental interactions, γ_d. Other parameters are $\gamma_{L,R} = 50$ meV, $\epsilon_F = \epsilon_G$.

[22] N. Amdursky, D. Marchak, L. Sepunaru, I. Pecht, M. Sheves, and D. Cahen, Adv. Mater. **26**, 7142 (2015).
[23] Y. Dubi and M. Di Ventra, Rev. Mod. Phys. **83**, 131 (2011).
[24] M. Paulsson and S. Datta, Phys. Rev. B **67**, 241403 (2003).
[25] F. Pauly, J. K. Viljas, and J. C. Cuevas, hys. Rev. B **78**, 035315 (2008).
[26] J. P. Bergfield and C. A. Stafford, Nano Lett. **9**, 3072 (2009).
[27] J. P. Bergfield, M. A. Solis, and C. A. Stafford, ACS Nano **4**, 5314 (2010).
[28] S. Y. Quek, H. J. Choi, S. G. Louie, and J. B. Neaton, ACS Nano **5**, 551 (2011).
[29] M. Bürkle, L. A. Zotti, J. K. Viljas, D. Vonlanthen, A. Mishchenko, T. Wandlowski, M. Mayor, G. Schn, and F. Pauly, Phys. Rev. B **86**, 115304 (2012).
[30] M. Bürkle, T. J. Hellmuth, F. Pauly, and Y. Asai, Phys. Rev. B **91**, 165419 (2015).
[31] T. Markussen, C. Jin, and K. S. Thygesen, Phys. Status Solidi B **250**, 2394 (2013).
[32] O. Karlström, M. Strange, and G. C. Solomon, J. Chem. Phys. **140**, 044315 (2014).
[33] F. Hüser and G. C. Solomon, J. Phys. Chem. C **119**, 14056 (2015).
[34] D. Z. Manrique, Q. Al-Galiby, W. Hong, and C. J. Lambert, Nano Lett. **16** , 1308 (2016).
[35] Y. Dubi and M. Di Ventra, Nano Lett. **9**, 97 (2009).
[36] B. C. Hsu, Y.-S. Liu, S. H. Lin, and Y.-C. Chen, Phys. Rev. B **83**, 041404(R) (2011).
[37] B. C. Hsu, C.-W. Chiang, and Y.-C. Chen, Nanotechnology **23**, 275401 (2012).
[38] M. Galperin, A. Nitzan, and M. A. Ratner, Mol. Phys. **106**, 397 (2008).
[39] O. Entin-Wohlman, Y. Imry, and A. Aharony, Phys. Rev. B **82**, 115314 (2010).
[40] J.-T. Lü, J.-S. Wang, P. Hedegard, and M. Brandbyge, Phys. Rev. B **93**, 205404 (2016).
[41] C. A. Perroni, D. Ninno, and V. Cataudella, J. Phys.: Condens. Matter **28**, 373001 (2016).
[42] B. K. Agarwalla, J. H. Jiang, and D. Segal, Phys. Rev. B **92**, 245418 (2015).
[43] B. K. Agarwalla, J. H. Jiang, and D. Segal, Beilstein J. Nanotechnol. **6**, 2129 (2015).
[44] L. Simine, W. J. Chen, and D. Segal, J. Phys. Chem. C **119**, 12097 (2015).
[45] J. Koch, F. von Oppen, Y. Oreg, and E. Sela, Phys. Rev. B **70**,

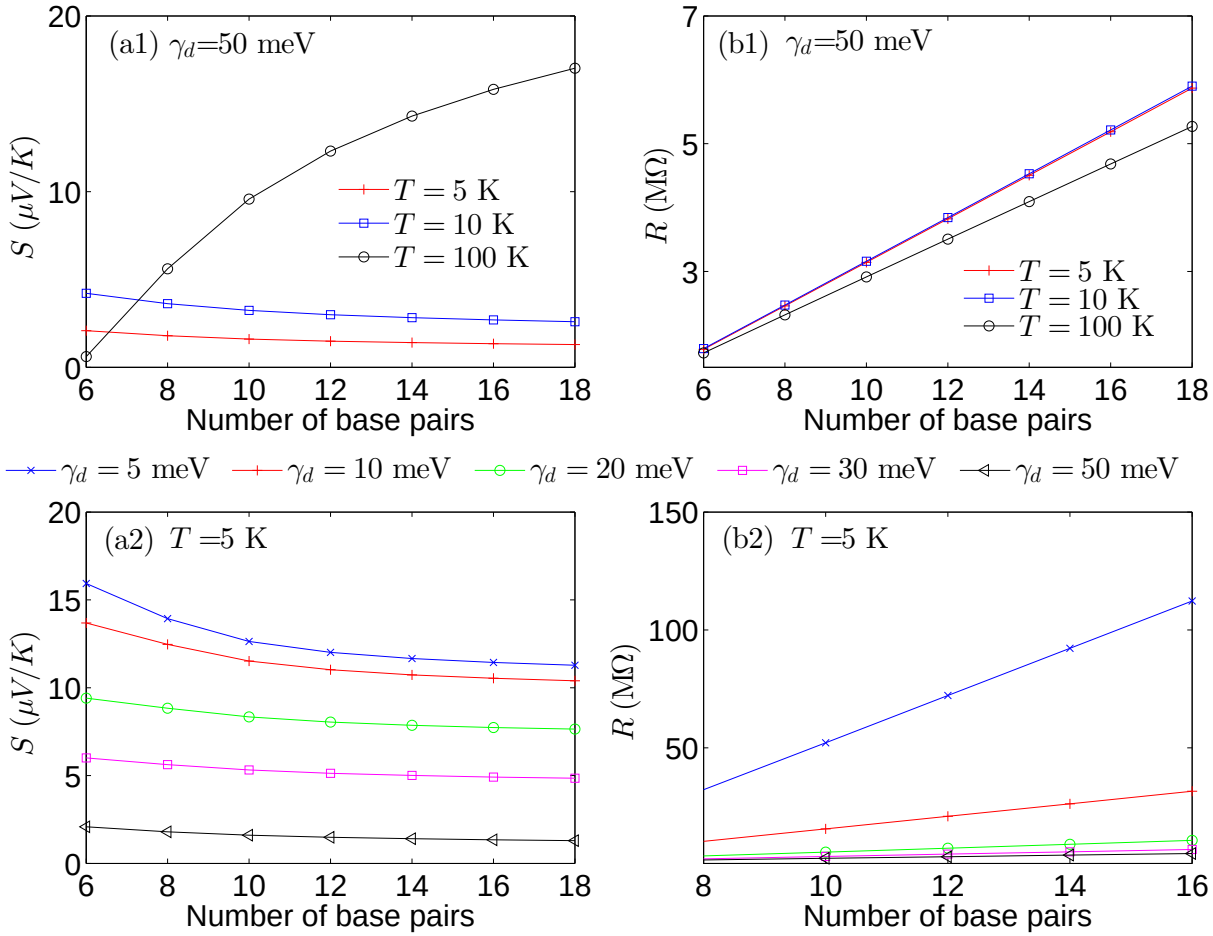

FIG. 10. (a) Thermopower and (b) electrical resistance of $(CG)_m$ sequences, see Table I, for a range of temperatures and environmental interactions γ_d. Other parameters are $\gamma_{L,R} = 50$ meV, $\epsilon_F = \epsilon_G$.

195107 (2004).
[46] K. Walczak, Physica B-Condensed Matter **392**, 173 (2007).
[47] D. Segal, Phys. Rev. B **72**, 165426 (2005).
[48] M. Büttiker, Phys. Rev. B **32**, 1846 (1985).
[49] M. Büttiker, Phys. Rev. B **33**, 3020 (1986).
[50] D. Nozaki, Y. Girard, and K. Yoshizawa, J. Phys. Chem. C **112**, 17408 (2008).
[51] D. Nozaki, C. Gomes da Rocha, H. M. Pastawski, and G. Cuniberti, Phys. Rev. B **85**, 155327 (2012).
[52] S. G. Chen, Y. Zhang, S. K. Koo, H. Tian, C. Y. Yam, G. H. Chen, and M. A. Ratner, J. Phys. Chem. Lett. **5**, 2748 (2014).
[53] R. Venkataramani, E. Wierzbinski, D. H. Waldeck, and D. N. Beratan, Faraday Discuss. **174**, 57 (2014).
[54] A. Dhar, Adv. Phys. **57**, 457 (2008).
[55] M. Bandyopadhyay and D. Segal, Phys. Rev. E **84**, 011151 (2011).
[56] K. Saaskilahti, J. Oksanen, and J. Tulkki, Phys. Rev. E **88**, 012128 (2013).
[57] M. Kilgour and D. Segal, J. Chem. Phys. **143**, 024111 (2015).
[58] M. Kilgour and D. Segal, J. Phys. Chem. C **119**, 25291 (2015).
[59] M. Kilgour and D. Segal, J. Chem. Phys. **144**, 124107 (2016).
[60] H. Kim, M. Kilgour, and D. Segal, arXiv:1607.08663
[61] P. A. Jacquet, J. Stat. Phys. **134**, 709 (2009).
[62] S. Bedkihal, M. Bandyopadhyay, and D. Segal, Euro. Phys. J. B **86**, 506 (2013).
[63] A. Shastry, and C. A. Stafford, arXiv:1603.00096.
[64] D. Roy and A. Dhar, Phys. Rev. B **75**, 195110 (2007).
[65] J. L. D'Amato and H. M. Pastawski, Phys. Rev. B **41**, 7411 (1990).
[66] J. Jortner, M. Bixon, T. Langenbacher, and M. E. Michel-Beyerle, Proc. Natl Acad. Sci. USA **95**, 12759 (1998).
[67] Y. A. Berlin, A. L. Burin, and M. A. Ratner, J. Am. Chem. Soc. **123**, 260 (2001).
[68] G. I. Livshits, A. Stern, D. Rotem, N. Borovok, G. Eidelshtein, A. Migliore, E. Penzo, S. J. Wind, R. Di Felice, S. S. Skourtis, J. C. Cuevas, L. Gurevich, A. B. Kotlyar, and D. Porath, Nat. Nanotechnol. **9**, 1040 (2014).
[69] N. V. Grib, D. A. Ryndyk, R. Gutierrez, and G. Cuniberti, J. Biophys. Chem. **1**, 77 (2010).
[70] C. Guo , K. Wang, E. Zerah-Harush, J. Hamill, B. Wang, Y. Dubi, and B. Xu, Nat. Chem. **8**, 484 (2016).
[71] M. Zilly, O Ujsaghy, and D. E. Wolf, Phys. Rev. B **82**, 125125 (2010).
[72] J. Qi, N. Edirisinghe, M. G. Rabbani, and M. P. Anantram, Phys. Rev. B **87**, 085404 (2013).
[73] A.-M. Guo and Q.-f. Sun, Phys. Rev. Lett. **108**, 218102 (2012).
[74] Y. Zhang, C. Liu, A. Balaeff, S. S. Skourtis and D. N. Beratan, Proc. Natl. Acad. Sci. U.S.A. **111**, 10049. (2014).

[75] P. Woiczikowski, T. Kubar, R. Gutierrez, R. Caetano, G. Cuniberti, and M. Elstner, J. Chem. Phys. **130**, 215104 (2009).
[76] M. H. Lee, S. Avdoshenko, R. Gutierrez, and G. Cuniberti, Phys. Rev. B **82**, 155455 (2010).
[77] R. Gutierrez, R. A. Caetano, B. P. Woiczikowski, M. Elstner, and G. Cuniberti, Phys. Rev. Lett. **102**, 208102 (2009).
[78] R. Gutierrez, R. Caetano, P. B. Woiczikowski, T. Kubar, M. Elstner, and G. Cuniberti, New J. Phys. **12**, 023022 (2010).
[79] C. Liu, L. Xiang, Y. Zhang, P. Zhang, D. N. Beratan, Y. Li, and N. Tao, Nat. Chem. (2016), DOI: 10.1038/nchem.2545.
[80] R. Gutierrez, S. Mohapatra, H. Cohen, D. Porath, and G. Cuniberti, Phys. Rev. B **74**, 235105 (2006).
[81] D. Brisker-Klaiman and U. Peskin, Phys. Chem. Chem. Phys. **14**, 13835 (2012).
[82] F. Grozema, Y. A. Berlin, and L. D. A. Siebbeles, J. Am. Chem. Soc. **122**, 10903 (2000).
[83] L. Xiang, J.L. Palma, C. Bruot, V. Mujica, M. A. Ratner, and N. Tao, Nat. Chem. **7**, 221 (2015).
[84] J. Yi, Phys. Rev. B **68**, 193103 (2003).
[85] D. Klotsa, R. A. Roemer, and M. S. Turner, Biophys. J. **89**, 2187 (2005).
[86] 5Wang, X. F.; Chakraborty, T. X. F. Wang and T. Chakraborty, Phys. Rev. Lett. **97**, 106602 (2006).
[87] K. Senthilkumar, F. C. Grozema, C. F. Guerra, F. M. Bickelhaupt, F. D. Lewis, Y. A. Berlin, M. A. Ratner, and L. D. A. Siebbeles, J. Am. Chem. Soc. **127**, 14894 (2005).